

Coherent Ising Machine - Optical Neural Network operating at the Quantum Limit -

Yoshihisa Yamamoto

ImPACT Program, Japan Science and Technology Agency,
K's Gobancho, 7, Gobancho, Chiyoda-ku, Tokyo 102-0076, Japan
E. L. Ginzton Laboratory, Stanford University, Stanford, CA 94305, USA
Fax: 81-3-6380-8263, e-mail: yyamamoto@stanford.edu

We will discuss the basic concept, operational principle and physical implementation of coherent Ising machines based on degenerate optical parametric oscillators. The developed coherent Ising machine with 2048 spins with all-to-all connections demonstrated already competitive performance against the state of art modern digital computers.

Key words: Ising machine, optical parametric oscillator, combinatorial optimization, dissipative quantum computation

1. INTRODUCTION

Combinatorial and continuous optimization problems are ubiquitous in our modern life. Classic examples include lead optimization in drug discovery and biocatalyst development, resource optimization in wireless communications, routing in power and transport network, scheduling, sparse coding in compressed sensing, Boltzmann sampling and deep learning in machine learning and portfolio optimization in fintech. Most of these optimization problems belong to Non-deterministic Polynomial (NP), NP-complete and NP-hard classes in complexity theory and modern digital computers based on von-Neuman architecture are not necessarily efficient for them. That is, the computational time scales exponentially when a problem size increases.

A gate-based or measurement-based quantum computer does not provide a valid solution for such combinatorial optimization problems, either. It is known that the optimum approach within a framework of quantum computing for such problems without hidden periodicity nor specific structure is given by Grover algorithm [1]. Table I shows the computation time by an ideal quantum computer based on Grover algorithm for NP-hard MAX-CUT problems with varying problem size $N = 20 \sim 150$. Here we assume a hypothetical quantum computer does not have any gate error nor decoherence, so that there is no need to employ resource-hungry quantum error correction. It is also assumed that all qubits are fully connected, so that there is no need to transfer qubit information over distant locations by resource-hungry swapping processes. Yet the computation time increases exponentially from $T_c = 4 \times 10^{-3}$ (s) for $N = 20$ (bits) to $T_c = 6 \times 10^{17}$ (s) or 20 billion years for $N = 150$ (bits). It is bad news that Grover algorithm is proven to be optimum for unstructured data search, so that there is no possibility to discover a more efficient algorithm unless the universality is given up.

If we go for a heuristic, which does not guarantee an exact solution for a really hard problem instance, there remains various possibilities to improve the computation time. One example along this line of quantum heuristic machines is the quantum approximate optimization algorithm (QAOA) which is implemented on the hybrid gate-based quantum computer and modern digital computer [2,3]. Another example for quantum heuristic machines is the Josephson qubit-based quantum annealing machine [4]. The computation time for those two machines are also shown in Table I, which are not competitive against the modern heuristic such as simulated annealing (SA) or breakout local search (BLS) implemented on CPU or GPU.

As shown in Fig. 1, we have proposed and implemented four quantum heuristic machines called, coherent Ising machine (CIM) [5-11], coherent SAT solver (CSS) [12], coherent XY machine (CXM) [13,14] and coherent crypto machine (CCM), to solve the NP-hard Ising problems, NP-complete k -SAT problems, continuous optimization problems and to perform secure (or private) computation of those problems, respectively. We use the optical parametric oscillators operating at the quantum limit to implement those four machines in quantum neural network.

Table I. Time-to-solution for NP-hard MAX-CUT problems by various quantum machines.

Problem Size	Universal Quantum Computers*	Heuristic Machines		
		QAOA-based Quantum Computer**	Quantum Annealer***	Coherent Ising Machine****
$N = 20$	4×10^{-3} (s)	600 (s)	1.1×10^{-5} (s)	1.0×10^{-4} (s)
$N = 50$	6×10^2 (s)	---	5.0×10 (s)	3.7×10^{-4} (s)
$N = 100$	2×10^{10} (s) (~700 years)	---	(~ 10^{17} (s))	2.5×10^{-3} (s)
$N = 150$	6×10^{17} (s) (~20B years)	---	(~ 10^{32} (s))	5.4×10^{-2} (s)

* Theoretical limit (no decoherence, no gate error, all-to-all connections, 1 nsec gate time)
 ** Rigetti Computing 19 bit machine (Quantum Approximate Optimization Algorithm, Dec. 2017)
 *** D-WAVE 2000Q (Experimental: $N = 20, 50$, Expected: $N = 100, 150$)
 **** NTT 2000 CIM with all-to-all connections (Experimental: $N = 20, 50, 100, 150$)

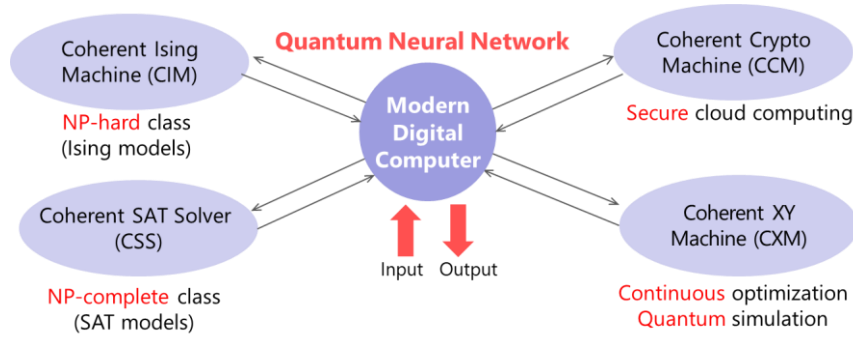


Fig. 1. Quantum neural networks for combinatorial and continuous optimization problems.

2. QUANTUM COMPUTATION MODELS

There are three quantum computational models proposed today: unitary quantum computation [15,16], adiabatic quantum computation [17,18] and dissipative quantum computation [19,20]. Table II compares the two quantum computational models. A gate-model or measurement-based quantum computer implements the unitary quantum computational model and is expected to solve efficiently those problems with hidden periodicity or specific structure, while a coherent Ising machine (CIM), coherent XY machine (CXM) and coherent SAT solver (CSS) implement the dissipative quantum computational model and is expected to feature a better performance for the unstructured optimization problems. The unitary quantum computation requires an enormous overhead for quantum error correction, but its theoretical limit is well established. The dissipative quantum computation is still far from complete understanding since it is based on the complicated physics of quantum Darwinism and quantum chaos, but it is attractively robust against noise and errors.

Table II. Two quantum computational models.

	Unitary quantum computation [15,16]	Dissipative quantum computation [19,20]
Realization	Gate-model/Measurement-based	Coherent Ising/XY/Recurrent machines
Principle	Unitary rotation of state vectors in a closed system	Self-stabilized ordering in an open system
Proposal	Deutsch (1985) : quantum parallelism Shor (1994) : quantum algorithm	Zurek (2003) : quantum Darwinism and quantum chaos Verstraete, Wolf, and Cirac (2008) : quantum algorithm
Pros	Transparent physics	Robust against noise and error
Cons	Vulnerable to noise and error	Complicated physics
Applications	Problems with hidden periodicity (factoring, discrete-logarithm)	Problems with no periodicity (optimization, sampling)

3. TWO TYPES OF CIMS

Table III compares the two types of CIMS, optical delay line coupling machine (DL-CIM) [7-9] and measurement feedback coupling machine (MF-CIM) [10,11]. Figure 2 shows the physical implementation of the two types of CIMS. In DL-CIM, all-to-all connections among N spins can be realized by $N-1$ optical delay lines with dynamic modulation of coupling constants. In MF-CIM, the same function can be achieved with a single measurement-feedback loop so that physical implementation of MF-CIM is more straightforward than DL-CIM. The DL-CIM is inherently an all-optical system and enjoys a high-speed operation. This machine can implement both classical and quantum Hamiltonians. Quantum parallel search mechanism of DL-CIM is quantum entanglement (correlation) among OPO pulses [21,22] and naturally fitted to find a many body ground state with quantum entanglement. The MF-CIM is an optical-electrical hybrid system and can implement a higher order Ising coupling such as three-body, four-body \dots interactions [23]. Quantum parallel search mechanism of MF-CIM is quantum walk enhanced by non-Gaussian OPO pulses [24,25] and naturally fitted to combinatorial optimization formulated by classical Hamiltonian.

Table III. Optical delay line coupling machine (DL-CIM) vs. Measurement-feedback coupling machine (MF-CIM).

	DL-CIM [7-9]	MF-CIM [10,11]
Implementation	$(N-1)$ optical delay lines with dynamic modulation based on $[J_{ij}]$	Single measurement-feedback loop consisting of homodyne detector, ADC-FPGA-DAC circuit and optical modulator
Quantum parallel search	Quantum entanglement	Quantum walk
Pros	<ul style="list-style-type: none"> ■ High-speed operation ■ Both classical and quantum Hamiltonians 	<ul style="list-style-type: none"> ■ Robust against optical loss and phase noise ■ High-order Ising couplings ($\sigma_1\sigma_2\sigma_3\dots$)
Cons	Sensitive to optical loss and phase error	Speed limit imposed by electronics
Applications	<ul style="list-style-type: none"> ■ Quantum simulation ■ Large-scale problems with regular/sparse connections 	<ul style="list-style-type: none"> ■ Classical Hamiltonian (combinatorial optimization) ■ Medium-scale problems with irregular/dense connections

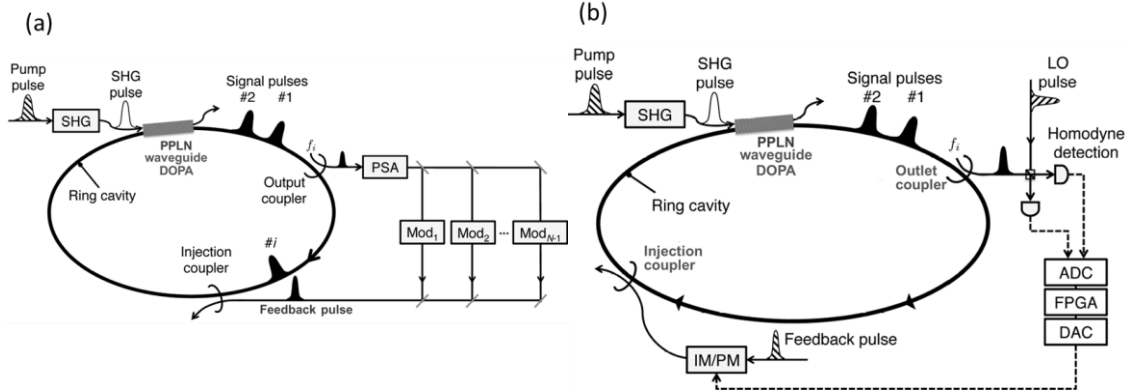


Fig. 2. (a) A coherent Ising machine (CIM) based on the time-division multiplexed DOPO pulses with mutual coupling implemented by optical delay lines. A part of each pulse is picked off from the main cavity by the output coupler followed by an optical phase sensitive amplifier (PSA) which amplifies the in-phase amplitude of the extracted DOPO pulse. The feedback pulses, which are produced by combining the outputs from $N-1$ intensity and phase modulators, are injected back to the target DOPO pulse by the injection coupler [7-9]. (b) A CIM with a measurement-feedback circuit. A small portion of each DOPO signal pulse is out-coupled through the output coupler, and its in-phase amplitude is measured by optical balanced homodyne detectors, where LO pulse is directly obtained from the pulsed pump laser. Two detector outputs are converted to digital signals and input into an electronic digital circuit, where a feedback signal for the i -th DOPO signal pulse is computed. The feedback pulse also taken from the pump laser is modulated in its intensity and phase to achieve the target feedback amplitude and coupled into the i -th signal pulse by an injection coupler. Flows of optical fields and electrical signals are shown as solid and dashed lines, respectively [10,11].

4. PERFORMANCE COMPARISON AGAINST QUANTUM COMPUTERS, QUANTUM ANNEALING MACHINES AND MODERN DIGITAL COMPUTERS

Table III summarizes the benchmark study results of the CIM vs. universal quantum computers, quantum approximate optimization algorithm (QAOA) machines and quantum annealing machines against NP-hard MAX-CUT problems [26]. The time-to-solution for the complete graph MAX-CUT problems, which are identical to the Sherrington-Kirkpatrick spin glass model with $N = 20, 50, 100$ and 150 spins, are listed for various approaches. The time-to-solution for a universal quantum computer based on Grover algorithm is a theoretical value, where an ideal quantum processor with no decoherence, no gate error and all-to-all direct coupling among qubits is assumed, so that any overhead for quantum error correction is not included. Therefore, it is considered as an absolute theoretical limit on the computation time. Yet, the computation time is 4×10^{-3} (s), 600 (s), 2×10^{10} (s) and 6×10^{17} (s) for $N = 20, 50, 100$ and 150 . This is an exponential scaling and traced back to the exponential time required to implement Grover algorithm which is proven to be optimum in the framework of unitary quantum computation. There are the experimental time-to-solution for three heuristic machines in Table I: Rigetti quantum approximate optimization algorithm (QAOA) machine [2,3], D-WAVE quantum annealing machine and NTT-CIM [26]. (It is noted that CIM features a far better performance than other quantum processors even when the problem size is relatively small.)

Figure 3 compares the time-to-approximate solution by CIM and modern supercomputer [27]. The problem is the Sherrington-Kirkpatrick spin glass model with $N = 2000$ spins. It is not possible to obtain an exact solution with any existing computer and algorithm for this size of NP-hard problems, so that we use the approximate solution by Goemans-Williamson Semi-Definite Programing (SDP) [28] as a target. The GW-SDP guarantees an accuracy better than 87.8% in the worst case. The NTT-CIM reaches this approximate solution in $\sim 70 \mu\text{sec}$, while the supercomputer (Shoubu) at Riken, Japan, returns the same solution in ~ 7 msec. We use the Hopfield-Tank neural network model as an algorithm for the supercomputer, since this model is a closest classical analog for CIM.

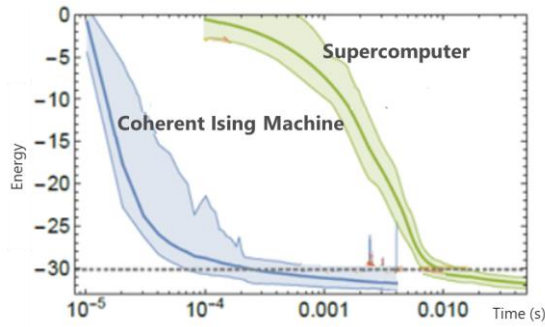


Fig. 3. Energy vs. time for coherent Ising machine and supercomputer against $N = 2000$ spin glass problem (SK model) [27].

Finally, Fig. 4 compares the error rates of CIM and best-known heuristic (Breakout Local Search: BLS) [29] for $N = 100, 200$ and 500 NP-hard MAX-CUT problems [12]. The CIM can achieve orders of magnitude smaller error rates than the state of art heuristic method. The computation time for CIM in Fig. 4 is a simulation time by standard desktop computers and real computation time in physical CIM is a factor 100~1000 smaller than the values shown in Fig. 4.

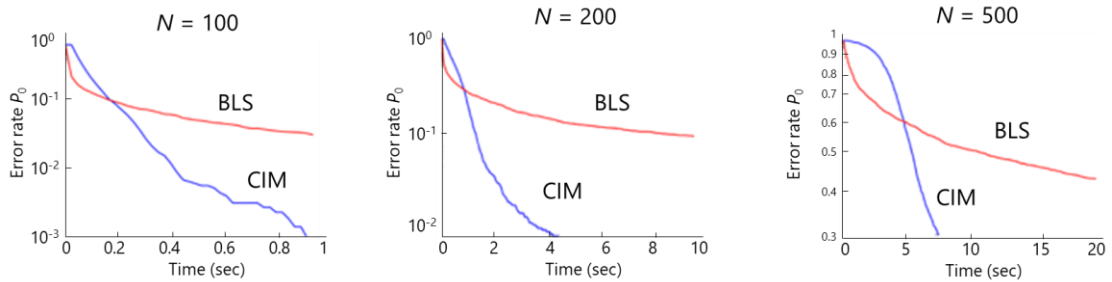


Fig. 4. The error rate in finding an exact solution vs. computation time for CIM and BLS [12]. The time for CIM is a simulation time by desktop computers and the real computation time of CIM is a factor 100~1000 smaller than those values.

ACKNOWLEDGMENT

This research was supported by ImPACT Program of Council for Science, Technology and Innovation (Cabinet Office, Government of Japan).

REFERENCES

- [1] L. K. Grover, Proc. 28th ACM Symposium on Theory of Computing, 212-219 (1996).
- [2] E. Farhi, J. Goldstone, S. Gutmann, and H. Neven, arXiv:1703.06199 (2017).
- [3] J. S. Otterbach, R. Manenti, N. Alidoust, A. Bestwick, M. Block, B. Bloom, S. Caldwell, N. Didier, E. S. Fried, S. Hong, P. Karalekas, C. B. Osborn, A. Papageorge, E. C. Peterson, G. Prawiroatmodjo, N. Rubin, C. A. Ryan, D. Scarabelli, M. Scheer, E. A. Sete, P. Sivarajah, R. S. Smith, A. Staley, N. Tezak, W. J. Zeng, A. Hudson, B. R. Johnson, M. Reagor, M. P. da Silva, and C. Rigetti, arXiv:1712.05771 (2017).
- [4] D-Wave Systems Inc., Technical description of the D-Wave quantum processing unit (2016). Part of D-Wave API documentation.
- [5] Z. Wang, A. Marandi, K. Wen, R. L. Byer, and Y. Yamamoto, Phys. Rev. A 88, 063853 (2013).
- [6] T. Leleu, Y. Yamamoto, S. Utsunomiya, and K. Aihara, Phys. Rev. E 95, 022118 (2017).
- [7] A. Marandi, Z. Wang, K. Takata, R. L. Byer, and Y. Yamamoto, Nature Photonics 8, 937-942 (2014).
- [8] K. Takata, A. Marandi, R. Hamerly, Y. Haribara, D. Maruo, S. Tamate, H. Sakaguchi, S. Utsunomiya, and Y. Yamamoto, Sci. Rep. 6, 34089 (2016).
- [9] T. Inagaki, K. Inaba, R. Hamerly, K. Inoue, Y. Yamamoto, and H. Takesue, Nature Photonics 10, 415-419 (2016).
- [10] T. Inagaki, Y. Haribara, K. Igarashi, T. Sonobe, S. Tamate, T. Honjo, A. Marandi, P. L. McMahon, T. Umeki, K. Enbutsu, O. Tadanaga, H. Takenouchi, K. Aihara, K. Kawarabayashi, K. Inoue, S. Utsunomiya, and H. Takesue, Science 354, 603-606 (2016).
- [11] P. L. McMahon, A. Marandi, Y. Haribara, R. Hamerly, C. Langrock, S. Tamate, T. Inagaki, H. Takesue, S. Utsunomiya, K. Aihara, R. L. Byer, M. M. Fejer, H. Mabuchi, and Y. Yamamoto, Science 354, 614-617 (2016).
- [12] T. Leleu et al., Phys. Rev. Lett (to appear).
- [13] S. Tamate, Y. Yamamoto, A. Marandi, P. McMahon, and S. Utsunomiya, arXiv:1608.00358 (2016).
- [14] Y. Takeda, S. Tamate, Y. Yamamoto, H. Takesue, T. Inagaki, and S. Utsunomiya, Quantum Sci. Technol. 3, 014004 (2018).
- [15] D. Deutsch, Proc. Royal Soc. (London) A 400, 97-117 (1985); D. Deutsch and R. Jozsa, Proc. Royal Soc. (London) A 439, 553-558 (1992).
- [16] P. W. Shor, Proc. of the 35th Annual Symposium on Foundations of Computer Science, IEEE Computer Society Press, 124-134 (1994).
- [17] E. Farhi, J. Goldstone, S. Gutmann, J. Lapan, A. Lundgren, and D. Preda, Science 292, 472-475 (2001).
- [18] T. Kadowaki and H. Nishimori, Phys. Rev. E 58, 5355 (1998).
- [19] W. H. Zurek, Rev. Mod. Phys. 75, 715-775 (2003).
- [20] F. Verstraete, M. M. Wolf, and J. I. Cirac, Nature Phys. 5, 633-636 (2009).
- [21] K. Takata, A. Marandi, and Y. Yamamoto, Phys. Rev. A 92, 043821 (2015).
- [22] D. Maruo, S. Utsunomiya, and Y. Yamamoto, Phys. Scr. 91, 083010 (2016).
- [23] S. Utsunomiya, K. Takata, and Y. Yamamoto, Optics Express 19, 18091-18108 (2011).
- [24] A. Yamamura, K. Aihara, and Y. Yamamoto, Phys. Rev. A 96, 053834 (2017).
- [25] T. Shojj, K. Aihara, and Y. Yamamoto, Phys. Rev. A 96, 053833 (2017).
- [26] R. Hamerly, T. Inagaki, P. L. McMahon, D. Venturelli, A. Marandi, T. Onodera, E. Ng, C. Langrock, K. Inaba, T. Honjo, K. Enbutsu, T. Umeki, R. Kasahara, S. Utsunomiya, S. Kako, K. Kawarabayashi, R. L. Byer, M. M. Fejer, H. Mabuchi, D. Englund, E. Rieffel, H. Takesue, and Y. Yamamoto, arXiv:1805.05217 (2018).
- [27] Y. Haribara, H. Ishikawa, S. Utsunomiya, K. Aihara, and Y. Yamamoto, Quantum Sci. Tech. 2, 044002 (2017).
- [28] M. X. Goemans and D. P. Williamson, J. ACM 42, 1115-1145 (1995).
- [29] U. Benlic and J. K. Hao, Eng. Appl. Artif. Intell. 26, 1162-1173 (2013).